

## RADIAL VELOCITY SPECTROMETER DESIGN AND PERFORMANCE

D. Katz\*

Observatoire de Paris, GEPI / CNRS UMR 8111, 92195 Meudon cedex, France

### ABSTRACT

The Radial Velocity Spectrometer (RVS) is an integral field spectrograph dispersing all the light entering its  $\sim 2.5 \times 1.6 \text{ deg}^2$  field of view, with a resolving power  $R = \lambda/\Delta\lambda = 11\,500$ . The wavelength range of the RVS, [848–874] nm, contains strong spectral features (Ca II triplet in intermediate and late-type stars and Hydrogen Paschen lines in early-type stars) as well as measurable weak lines (e.g., Si I or Mg I). The RVS will collect the spectra of about 100–150 million stars down to magnitude  $V \simeq 17$ –18. Each source will be observed on average, at 93 successive epochs. The main aim of the RVS is the acquisition of the radial velocities. As third components of the velocity vectors, the radial velocities are crucial to study the kinematical and dynamical history of the Milky Way. Multi-epoch radial velocities will also be very useful to identify and characterise double and multiple systems. Moreover, the radial velocities are necessary to correct the astrometric measurements from perspective acceleration. The RVS should derive radial velocities with precisions, at the end of the mission, for e.g., a solar metallicity G5 dwarf, of  $\sim 3.5 \text{ km s}^{-1}$  at  $V = 16$  and  $\sim 9.5 \text{ km s}^{-1}$  at  $V = 17$ . The RVS will also provide rotational velocities, atmospheric parameters, individual abundances, interstellar reddening as well as numerous stellar diagnostics (e.g., variability, mass loss).

Key words: Gaia; Space vehicles: instruments; Instrumentation: spectrographs; Techniques: spectroscopic; Techniques: radial velocities.

### 1. INTRODUCTION

The main objective of the Gaia mission (Perryman et al. 2001; Mignard 2005; Perryman 2005) is to identify and understand the mechanisms of formation and evolution of the Milky Way. The keys to decipher the Galaxy history are contained in its present day spatial, kinematical and chemical structure. The three complementary instruments of Gaia will provide the information to map these distributions. The astrometric instrument will determine the coordinates, distances, absolute magnitudes (surface

gravities through modelling) and proper motions. The Broad and Medium-Band Photometers will constrain the stellar atmospheric parameters as well as the 3D map of the interstellar reddening. The Radial Velocity Spectrometer (RVS) will provide the radial velocities as well as stellar and interstellar parameters.

The acquisition of radial velocities for the largest possible number of Gaia targets constitute the first goal of the RVS. As third components of the velocity vectors, the radial velocities are crucial to study, without *a priori* assumptions, the kinematical properties of the Galaxy. The radial velocities are also necessary to correct the astrometric measurements of  $\sim 10^5$  ‘nearby’ stars (Arenou & Haywood 1998) from perspective acceleration: a time quadratic apparent displacement induced by the motion of the source along the line of sight. Finally, multi-epoch radial velocities will be very useful for spotting transient phenomena and for detecting and characterising multiple systems (Söderhjelm 2005) and variable stars.

The RVS wavelength range contains a mix of strong and weak lines from different chemical species. This variety of spectral transitions will provide several stellar and interstellar parameters in addition to the radial velocities: rotational velocities, atmospheric parameters<sup>1</sup> (effective temperature, surface gravity, metallicity), individual abundances of several key tracers of the chemical history of the Galaxy (e.g., Si, Mg) and diagnostics of ‘particular’ stellar behaviours: e.g., mass loss. The RVS domain also contains a Diffuse Interstellar Band (DIB) located at 862 nm, which, unlike other known DIBs, appears to be a reliable tracer of interstellar reddening (Munari 1999, 2000). The DIB will complement the photometric observations for the derivation of the map of the Galactic interstellar reddening.

The following sections review the different facets of the Radial Velocity Spectrometer: instrument design (Section 2), spectra (Section 3), performance (Section 4), expected scientific yield (Section 5) and on-ground data treatment (Section 6). A more detailed description of the instrument design and performance can be found in Katz et al. (2004). Some information (e.g., RVS CCD assembly) presented in the present article have been updated with respect to Katz et al. (2004) to account for some

\* On behalf of the Radial Velocity Spectrometer Working Group, see <http://wwwwhip.obspm.fr/gaia/rvs/members.html>

<sup>1</sup>The atmospheric parameters will be derived using jointly the astrometric, photometric and spectroscopic information.

small modifications of the design. The RVS main technical issues as well as the RVS on-board processing are discussed in Cropper et al. (2005). A detailed synthesis of the RVS expected scientific harvest is given in Wilkinson et al. (2005). Many articles in the present proceedings are devoted to the RVS performance and scientific capabilities. They draw a broad overview of the RVS technical and scientific cases.

## 2. RVS DESIGN

### 2.1. Design Overview

The RVS is a near infrared ([848–874] nm) medium resolution ( $R = \lambda/\Delta\lambda = 11\,500$ ) spectrograph. It is a slitless and fiberless integral field instrument, dispersing all the light entering its  $\sim 2.5 \times 1.6 \text{ deg}^2$  field of view. As with the other Gaia instruments, the RVS will repeatedly scan the celestial sphere. During the 5 years of the mission, a source will be observed, on average, at 93 epochs.

### 2.2. Optics

The Medium-Band Photometer (MBP) and the RVS are illuminated by the same telescope (hereafter referred to as Spectro telescope). The first half of the field of view of the Spectro telescope is only imaged on the MBP. The second half is imaged on both the MBP and the RVS. A beam-splitter separates the blue wavelengths, which are transmitted to the MBP, from the red wavelengths, which are reflected toward the RVS. The Spectro telescope has a collecting area of  $\sim 0.25 \text{ m}^2$  and a focal length of 2.3 m.

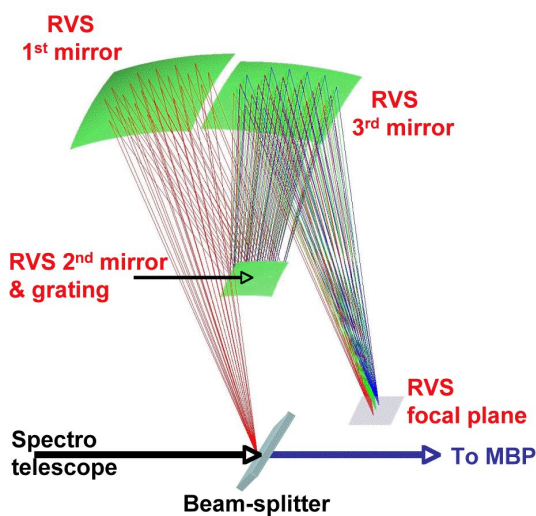


Figure 1. Schematic view of the RVS and its environments. The light coming from the Spectro telescope is separated by a beam-splitter into a ‘blue’ beam transmitted to the MBP and a ‘red’ beam reflected toward the mirrors of the RVS.

As shown on Figure 1, the RVS optical design is based on the Offner relay concept. It is a purely reflective system (without dioptric element) made of three mirrors. A grating, ruled on the secondary mirror, disperses the light. The spectral dispersion is oriented along the scan direction. A filter (whose location is not yet defined) will restrict the wavelength to the RVS domain ([848–874] nm) and will block the secondary spectral orders. The RVS has a focal length of 2.3 m.

### 2.3. Spectro Focal Planes

As illustrated by Figure 2, a source entering the Spectro telescope field of view is first recorded by a group of 20 MBP CCDs distributed in 2 rows of 10 detectors each (hereafter referred to as MBP-red, because they contain the red MBP bands). After the crossing of the MBP-red detectors, the light is divided by a beam-splitter into a blue and a red component. The blue component crosses a second group of 20 MBP-CCDs (called MBP-blue), while the red component is dispersed by the Offner Relay and crosses the RVS CCDs.

### 2.4. Spectro Sky-mappers & RVS Photometric Band

Contrary to Hipparcos, Gaia will use no input catalogue. Yet, in order that the data stream fits within the telemetry budget, only the pixels containing sources (e.g., asteroids, stars, galaxies) will be transmitted to the ground. The sources will be detected on-board Gaia, in real time, by dedicated detectors named sky-mappers.

The MBP and RVS instruments share the same set of sky-mappers (hereafter referred to as Spectro sky-mappers). As shown on Figure 2, the Spectro sky-mappers are integrated within the MBP-red detectors. The detection process is first performed two times (by SSM1 and SSM2). The two detection diagnostics are compared to discriminate between true (i.e., source) and false (e.g., cosmic rays, defective pixels) detections. Once a detection is validated, the information is transmitted to all the detectors that will be crossed by the source (i.e., MBP-red, MBP-blue and RVS CCDs) in order that only the ‘relevant’ pixels be transferred to the ground. The detection process is then repeated two times (by SSM3 and SSM4) to identify and characterise moving objects (i.e., asteroids). The sky-mappers are not filtered, but are illuminated in white light to maximise the sources signal to noise ratios and thus to improve the detection threshold. The Astro and Spectro detection processes are described in detail in Arenou et al. (2005).

Two of the red-MBP CCDs are filtered with the same filter as the RVS instrument. These ‘RVS magnitudes’ are used on-board, together with the information provided by the sky-mappers, to select the sources whose spectra should be transmitted to the ground (e.g., spectra of ‘very faint’ stars, for which no ‘accurate’ radial velocity can be derived, will not be sent to Earth). The ‘RVS magnitudes’ will also be used, subsequently on the ground, to calibrate and analyse the spectroscopic data.

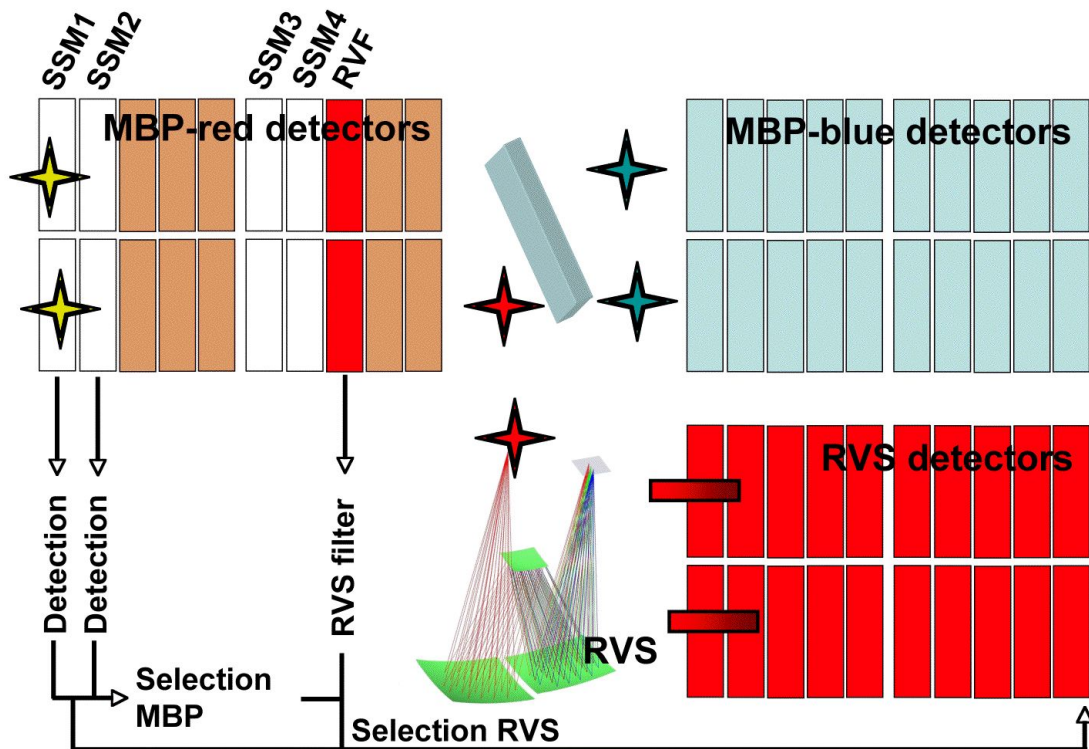


Figure 2. Schematic view of the MBP and RVS instruments. SSM 1 to 4 are the 4 sky-mappers and RVF is the photometric band which is filtered with the same filter as the RVS. The sources first cross (from left to right on the figure) the ‘MBP-red’ CCDs, where they are detected by the sky-mappers. The ‘blue’ and ‘red’ wavelengths are then separated by a beam-splitter. The ‘blue’ component crosses the ‘MBP-blue’ CCDs, while the ‘red’ one is dispersed by the RVS and crosses the RVS CCDs.

## 2.5. RVS Focal Plane

The RVS focal plane is made of 20 CCDs grouped in 4 modules of 5 CCDs each and distributed on two rows of 2 modules each. The RVS detectors are CCDs of ‘Low Light Level’ (L3) type. This relatively recent technology has been used for some years in ground observations. It is currently in space qualification phase for use on-board Gaia. The L3 CCDs are equipped with a signal amplifier system, which reduces the relative contribution of the readout noise. The RVS L3 CCDs will be operated with a moderate gain,  $G = 10$ . This gain will reduce the total electronic noise to  $2e^-$  per pixel. Table 1 summarises the characteristics of the RVS focal plane and detectors.

As the other Gaia detectors, the RVS CCDs are operated in Time Delay Integration (TDI) mode: i.e., the charges are shifted along scan by one pixel every 14.94 ms, to follow the sources in their crossing of the focal plane. The last column of each CCD is read at each TDI period.

The 10 CCDs (on each row) are scanning the same strip of sky (with small shifts in time). To reduce the telemetry flux, the 10 streams of data are corrected for cosmic rays and defective pixels, remapped on a common frame and coadded on-board, before transmission to the Earth. The on-board processing of the spectroscopic data is described in detail in Cropper et al. (2005).

Table 1. Characteristics of the RVS focal plane and CCDs. Some quantities (such as CCD dimensions) are still in optimisation phase and their values may still slightly change over the next few months.

Focal plane dimensions	$2.46 \times 1.60 \text{ deg}^2$
Focal plane effective area	$2.30 \times 1.47 \text{ deg}^2$
Focal plane crossing time	148 s
Number of CCDs	$10 \times 2$
CCD type	Low Light Level (L3)
Operating mode	Time Delay Integration
CCD dimensions	$923 \times 3930 \text{ pixel}$
CCD dimensions	$0.23 \times 0.74 \text{ deg}^2$
Exposure per CCD	13.8 s
Pixel dimensions	$10 \times 15 \mu\text{m}^2$
Pixel dimensions	$0.9 \times 1.35 \text{ arcsec}^2$

## 3. RVS SPECTRA

In late-type stars, the ionised Calcium triplet (849.80, 854.21, 866.21 nm) is the dominant feature in the RVS wavelength range (848–874 nm). The intensity of the Calcium triplet decreases with surface gravity, but remains very strong in dwarf stars. RVS spectra also contain many weak unblended (or moderately blended) lines

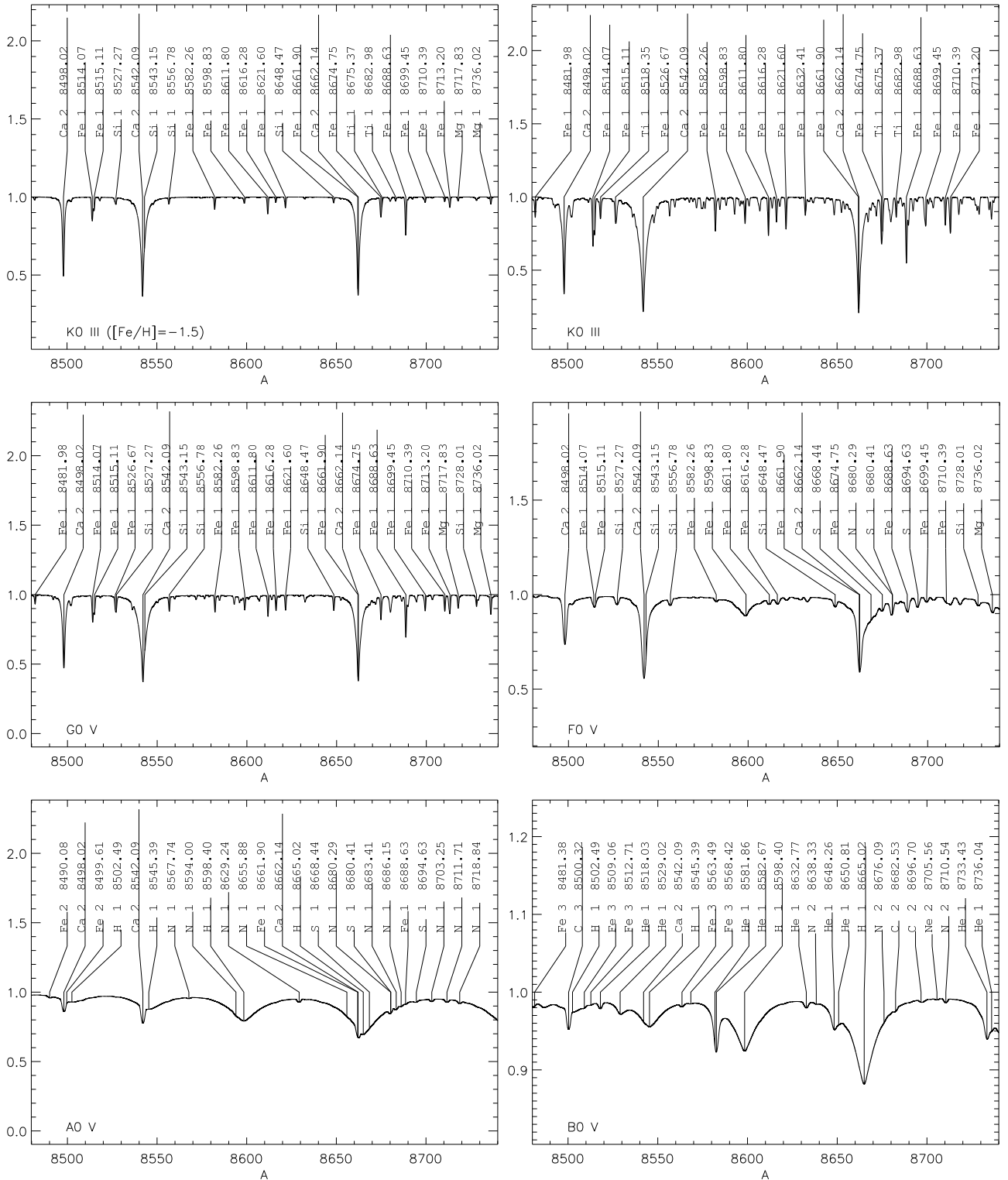


Figure 3. Examples of spectra in the RVS wavelength range: a metal-poor K0 III (top left) and a K0 III (top right), a G0 V (middle left), an F0 V (middle right), an A0 V (bottom left) and B0 V (bottom right) of solar metallicities.

of different chemical species and in particular of some alpha elements: e.g., Si I, Mg I. The spectra of the coolest stars exhibit no strong molecular bandhead, but many molecular transitions of CN and TiO are visible.

The spectra of early-type stars are dominated by lines of the end of the Hydrogen Paschen series. The intensities

of these lines also decrease with gravity. Other lines are also present in the spectra of hot stars: e.g., Ca II, N I, He I and He II.

Figure 3 shows examples of spectra in the RVS wavelength range, a metal-poor K0 III and five solar metallicity stars: a K0 III, a G0 V, an F0 V, an A0 V and

a B0 V. The six spectra are synthetic spectra computed using Kurucz atmospheric model (Kurucz 1993a), the VALD atomic data (Piskunov et al. 1995; Ryabchikova et al. 1999; Kupka et al. 1999) and N. Piskunov SYNTH program (Piskunov 1992). Table 2 summarises the stellar parameters used to compute the synthetic spectra.

Table 2. Stellar parameters used to compute the synthetic spectra presented in Figure 3.

	$T_{\text{eff}}$ (K)	$\log g$	$[Fe/H]$ (dex)	$[\alpha/Fe]$ (dex)	$v \sin i$ ( $\text{km s}^{-1}$ )
K0 III MP	4650	2.0	-1.5	+0.4	5
K0 III	4650	2.0	0.0	0.0	5
G0 V	5950	4.5	0.0	0.0	5
F0 V	7300	4.5	0.0	0.0	50
A0 V	9800	4.5	0.0	0.0	50
B0 V	30000	4.0	0.0	0.0	50

## 4. PERFORMANCE

### 4.1. Radial Velocities

The acquisition of ‘accurate’ and precise radial velocities for the largest possible number of stars is the primary goal of the Radial Velocity Spectrometer. Table 3 presents the RVS radial velocity precisions as a function of magnitude, for four different stellar types: a metal-poor K1 III and a K1 III, a G5 V and an A0 V of solar metallicities. As for similar earlier studies (Katz 2000; Munari et al. 2001; Zwitter 2002; David 2002), the performances have been evaluated by the Monte-Carlo method. For each stellar type and each magnitude, 500 to 1000 (500 for the bright stars to 1000 for the faint ones) RVS-like spectra have been simulated. Their radial velocities have been derived, by cross-correlation in direct space with a synthetic reference spectra. The standard deviations of the distributions of radial velocity errors (recovered minus true radial velocities) multiplied by a *safety margin* (see below) have been adopted as a measure of the radial velocity precisions.

To simulate RVS-like spectra, high resolution ( $R = 250\,000$ ) Kurucz synthetic spectra (Kurucz 1993b) have been convolved with a Gaussian profile to the RVS resolving power and have been resampled with 2 pixels per resolution element. The spectra have been renormalised according to the source atmospheric parameters, its apparent magnitude and the RVS characteristics (e.g., collecting area, telescope reflective index, CCD quantum efficiency). The photon counts have been generated following a Poisson law and the zodiacal light (assuming a surface brightness of  $V = 21.75 \text{ mag arcsec}^{-2}$ ) and electronic noise have been added. The spectra have been generated CCD by CCD, transit by transit and have been co-added.

Many effects are not yet taken into account in the simulations: e.g., realistic PSF profile, CCD charge trapping-detraping, wavelength calibration error. In order to ac-

count for those currently missing effects in the assessment of the radial velocity performance, the standard deviations of the distributions of radial velocity errors are multiplied by a *safety margin* of 1.4. This factor is already included in Table 3.

### 4.2. Crowded Fields

The RVS is an integral field spectrograph. As a consequence, the spectra of ‘close’ neighbours will overlap. At high and intermediate Galactic latitudes, this phenomenon will have little impact on the performance (the precisions presented in Table 3 are representative of these latitudes). On the contrary, in the dense fields of the disc and bulge, the spectra overlapping rate will become very high and will affect the RVS performance.

In the crowded areas, the ‘background’ of each source will be made of the zodiacal light plus the superposition of the spectra of the neighbouring objects. At each successive observation of the same source, the spectrograph will scan the sky with a different orientation. Therefore, at each transit, the source will be perturbed by different neighbours. As a consequence, neighbouring objects with magnitudes fainter than  $V \simeq 14\text{--}15$  will add mainly a few photons of background and only very weak spectral signatures. Brighter stars will also add visible spectral features to the composite background, which will make the analysis more difficult.

Zwitter (2003) has shown that, if one knows the neighbours positions, spectral types, magnitudes and radial velocities, it is then possible to model and subtract the composite background. Positions, spectral types and magnitudes will be provided by the astrometric and photometric instruments. Radial velocities are less straightforward to obtain. They are at the same time necessary to model the background and unknown characteristics that should be extracted from the spectra. A probable way to solve this ‘problem’ (which will be demonstrated in forthcoming studies) is to proceed iteratively. The stars are analysed from the brightest to the faintest: i.e., their background is modelled and subtracted and their radial velocities are derived. The full process (background modelling/subtraction/radial velocity derivation of all sources) is repeated until convergence. At the first iteration, the background of a given star is modelled knowing the radial velocities of the sources brighter than this star (which have already been analysed), but not of the fainter stars. At the first iteration, these ‘faint’ perturbers can be represented by an average continuum (this do not require to know the radial velocity). From the second iteration, an estimate of the radial velocities of all sources/perturbers has been obtained and their spectral features can be ‘properly’ placed in the composite background.

Zwitter (2003) has performed a first assessment of the impact of crowding on the radial velocity performance. Up to  $\sim 20\,000 \text{ stars deg}^{-2}$  with  $V \leq 17$ , the crowding has only a minor impact on the performance.

Table 3. RVS radial velocity precisions, as a function of magnitude, for a single transit and at the end of the mission.

Type	$[Fe/H]$	$[\alpha/Fe]$	Single transit precisions ( $\text{km s}^{-1}$ )				End of mission precisions ( $\text{km s}^{-1}$ )			
			$V = 11$	$V = 13$	$V = 14.5$	$V = 15.5$	$V = 14$	$V = 16$	$V = 17$	$V = 18$
K1 III	-1.5	+0.4	$\leq 1$	2.3	7.3	21.5	$\leq 1$	2.7	6.7	24.7
K1 III	0.0	0.0	$\leq 1$	1.5	4.5	10.7	$\leq 1$	1.6	4.2	12.0
G5 V	0.0	0.0	$\leq 1$	2.9	9.2	—	$\leq 1$	3.4	9.4	—
A0 V	0.0	0.0	11.5	—	—	—	10.8	—	—	—

### 4.3. Other Stellar and Interstellar Parameters

In addition to the radial velocities, the RVS spectra also contain information on rotational velocities, atmospheric parameters, individual abundances, interstellar reddening and many other stellar diagnostics (e.g., mass loss). Table 4 reviews the limiting magnitude and the number of stars for which these stellar parameters will be provided by the RVS. The methods foreseen to derive the rotational velocities and the atmospheric parameters as well as the performance expected are described in dedicated articles in this volume: rotational velocities (Gomboc & Katz 2005), atmospheric parameters (Recio-Blanco et al. 2005; Zwitter et al. 2005).

Table 4. Limiting magnitudes and number of stars for which the RVS will provide radial velocities, rotational velocities, atmospheric parameters and individual abundances.

	$V_{\text{lim}}$	$N_{\text{stars}}$
Radial velocities	17–18	$100\text{--}150 \times 10^6$
Rotational velocities	15–16	$25\text{--}50 \times 10^6$
Atmospheric parameters	14–15	$10\text{--}25 \times 10^6$
Abundances (e.g., Si, Mg)	12–13	$2\text{--}5 \times 10^6$

## 5. EXPECTED SCIENTIFIC HARVEST

The RVS expected scientific harvest spans a large domain from Galactic structure to stellar physics. A detailed review is given in Wilkinson et al. (2005) as well as by the many articles which are devoted to the Gaia science case in the present proceedings. This section presents a few examples of RVS expected scientific yields.

The RVS will determine the radial velocities of K giants with precisions better than  $\sim 10 \text{ km s}^{-1}$  up to  $\sim 20 \text{ kpc}$ . Combined with the astrometric data, these velocities will be used to identify relics of past accretions of satellite galaxies and to constrain the mechanisms of formation of the Milky Way halo (Helmi & de Zeeuw 2000). The RVS will also probe the kinematics of a part of the outer halo with, e.g., stars at the tip of the red giant branch (RGB), with asymptotic giant branch stars (AGB) and with CH-type carbon stars, which will be observable up to  $\sim 50\text{--}75 \text{ kpc}$ . This large, complete and unbiased sample of remote tracers will allow to refine significantly the estimate of the mass of the Milky Way halo (Wilkinson & Evans

1999; Wilkinson 2005). The RVS spectra will also provide information on the kinematics of the spiral arms and of the young stellar population of the disc. Precisions better than  $\sim 5 \text{ km s}^{-1}$  will be obtained for B5V stars up to  $\sim 2.5 \text{ kpc}$  and for Cepheids up to the edge of the disc.

The RVS will provide individual abundances (e.g., Mg, Si, Ti) for  $\sim 2\text{--}5 \times 10^6$  stars down to  $V \simeq 12\text{--}13$ . This will allow the study of the chemical history of dwarf stars within a radius of a hundred to a few hundreds parsecs, e.g.,  $\sim 300 \text{ pc}$  for a G5 dwarf, and of giant stars up to several kiloparsecs, e.g.,  $\sim 2.5 \text{ kpc}$  for a K1 giant (see also Nissen 2005). The RVS will also contribute to the search of extremely metal-poor stars (Spite 2005). It will be able to identify stars with  $[Ca/H] < -4.0 \text{ dex}$  up to several kiloparsecs.

The RVS will observe about  $10^6$  spectroscopic binaries and about  $10^5$  eclipsing binaries. Of these  $10^5$  eclipsing binaries, about 25% will be double-lined spectroscopic binaries (SB2), for which it will be possible to derive the masses of the two components (Söderhjelm 2005). Multi-epoch radial velocities will also be very useful to monitor the radial velocity pulsations of variable stars. For example, radial velocities of classical Cepheids will be derived with precisions per epoch of  $\sim 5 \text{ km s}^{-1}$  from about ten to several tens of kiloparsecs (according to the Cepheid period/intrinsic luminosity).

## 6. ON-GROUND CALIBRATION AND ANALYSIS OF THE SPECTRA

During the 5 years of the mission, Gaia will collect about  $\sim 10^{12}$  astrometric measures,  $\sim 2 \times 10^{12}$  photometric measures and  $\sim 1.5 \times 10^{10}$  spectra. The huge number of stars observed by Gaia (one billion for astrometry and photometry and 100 to 150 millions for spectroscopy) will span ‘all’ stages of stellar evolution and will include most types of variable, peculiar, cataclysmic, binary and multiple systems. The huge amount of data and their heterogeneity require the development of new, optimised, robust and fully automated calibration and analysis algorithms.

The implementation of the Gaia data archiving, calibration and analysis system is one of the challenges of the mission. Since 2000, a prototype is developed in the context of the *Gaia Data Access and Analysis Study*, GDAAS (Torra 2005). The prototype is used to define and test the numerical data model, the data input/output

processes, the calibration of the satellite attitude, the calibration and analysis of the astrometric data (Lindegren 2001; Figueras 2005) as well as several data analysis algorithms (Ansari 2005).

## 6.1. Calibrations

The RVS, as the other Gaia instruments, will be operated in relatively ‘unusual’ conditions: it will continuously scan the sky during 5 years, it will observe  $100\text{--}150 \times 10^6$  stars at  $\sim 93$  different epochs (on average) and it will be thermally, mechanically and optically extremely stable. These factors should all together allow the RVS to iteratively auto-calibrate itself.

Among the millions of stars observed by the RVS, there will be a subset of stars which will be astrometrically, photometrically and spectroscopically very stable during the 5 years of observation. Those stars will be monitored, by the three instruments, all along the mission. Changes in their measured properties will trace the evolution of the instrumental characteristics. Therefore, using the Gaia observations of these stable reference stars it should be possible to self-calibrate the RVS. The RVS calibration philosophy is based on the pioneering work of Lindegren (2001) for the calibration of the astrometric instrument.

The RVS self-calibration will comprise three phases: (i) the characterisation of the stars (e.g., radial velocity), (ii) the identification and selection of stable reference sources and (iii) the calibrations of the instrument (e.g., spectral dispersion law) using the self-selected reference stars. The three steps will be iterated until convergence.

## 6.2. Data analysis

The RVS observations will be very heterogeneous. They will include ‘all’ spectral types and luminosity classes, most types of variable, peculiar, cataclysmic and multiple systems. They will present very different signal to noise ratios and very different levels of contamination by neighbouring sources (see Section 4.2). The number of epochs of observation will vary with the location of the sources on the sky. The merits and drawbacks of existing analysis techniques will be assessed as a function of the different observing conditions in order to determine the best suited to each case. When needed new methods will be developed.

Astrometry, photometry and spectroscopy will all three provide constraints on stellar surface gravities. Photometry and spectroscopy will also carry information on effective temperatures, metallicities, alpha elements abundances and interstellar reddening. In these cases, new methods will be developed to combine ‘optimally’ the information from the different Gaia instruments.

## ACKNOWLEDGMENTS

I would like to thank the RVS scientific and technical community as well as the ESA and industry teams for their involvement in the definition and optimisation of the Radial Velocity Spectrometer. I am very grateful to R. Kurucz, F. Kupka, N. Piskunov and the VALD people for making their software packages and molecular data available to the community.

## REFERENCES

- Ansari S., 2005, ESA SP-576, this volume
- Arenou F., Haywood M., 1998, Gaia technical report SWG-OPM-001
- Arenou F., Babusiaux C., Chéreau F., Mignot S., 2005, ESA SP-576, this volume
- Cropper M., Katz D., Holland A., et al., 2005, ESA SP-576, this volume
- David M., 2002, Gaia technical report RVS-MD-003
- Figueras F., 2005, ESA SP-576, this volume
- Gomboc M., Katz D., 2005, ESA SP-576, this volume
- Helmi A., de Zeeuw P.T., 2000, MNRAS, 319, 657
- Katz D., 2000, PHD thesis, University of Paris VII
- Katz D., Munari U., Cropper M., et al., 2004, MNRAS, in press
- Kupka F., Piskunov N., Ryabchikova T.A., Stempels H.C., Weiss W.W., 1999, A&AS, 138, 119
- Kurucz R., 1993a, ATLAS9 Stellar Atmosphere Programs and 2 km/s grid. Smithsonian Astrophysical Observatory, Cambridge, MA, CD-ROM No. 13, 13
- Kurucz R., 1993b, SYNTHE Spectrum Synthesis Programs and Line Data. Smithsonian Astrophysical Observatory, Cambridge, MA, CD-ROM No. 18, 18
- Lindegren L., 2001, , Gaia technical report GAIA-LL-34
- Mignard F., 2005, ESA SP-576, this volume
- Munari U., 1999, Baltic Astronomy, 8, 73
- Munari U., 2000, In: Porceddu I., Aiello S., eds, Proc. Ita. Phys. Soc. Conf. Vol. 67, Molecules in Space and in the Laboratory. Carloforte, p179 (also astro-ph/0010271)
- Munari U., Agnolin P., Tomasella L., 2001, Baltic Astronomy, 10, 613
- Nissen P., 2005, ESA SP-576, this volume
- Perryman M.A.C., 2005, ESA SP-576, this volume
- Perryman M.A.C., de Boer K.S., Gilmore G., et al., 2001, A&A, 369, 339
- Piskunov N.E., 1992, In: Glagolevskij Y.V., Romanuk I.I., eds, Stellar Magnetism. Nizhnij Arkhyz, p92
- Piskunov N.E., Kupka F., Ryabchikova T.A., Weiss W.W., Jeffery C.S., 1995, A&AS, 112, 525
- Recio-Blanco A., Bijaoui A., de Laverny P., Katz D., Thévenin F., 2005, ESA SP-576, this volume

- Ryabchikova T., Piskunov N., Stempels H., Kupka F., Weiss W., 1999, In: 6th International Colloquium on Atomic Spectra and Oscillator Strengths, Victoria BC, Canada, 1998, Physica Scripta, vol. 83, p162
- Söderhjelm S., 2005, ESA SP-576, this volume
- Spite M., 2005, ESA SP-576, this volume
- Torra J., 2005, ESA SP-576, this volume
- Wilkinson M.I., 2005, ESA SP-576, this volume
- Wilkinson M.I., Evans N.W., 1999, MNRAS, 310, 645
- Wilkinson M.I., Vallenari A., Turon C., et al., 2005, MNRAS submitted
- Zwitter T., 2002, A&A, 386, 748
- Zwitter T., 2003, In: Munari U., ed., ASP Conf. Ser. Vol. 298, GAIA Spectroscopy , Science and Technology. Astron. Soc. Pac., Monte-Rosa., 493
- Zwitter T., Munari U., Siebert A., 2005, ESA SP-576, this volume